Randomly Hyperbranched Polymers

Dominik Konkolewicz,[1] Robert G. Gilbert,[2] and Angus Gray-Weale[1]

[1]*School of Chemistry F11, University of Sydney, Sydney, NSW 2006, Australia*
[2]*Hartley Teakle Building, University of Queensland, Brisbane, QLD 4072, Australia*
(Received 3 January 2007; published 4 June 2007)

We describe a model for the structures of randomly hyperbranched polymers in solution, and find a logarithmic growth of radius with polymer mass. We include segmental overcrowding, which puts an upper limit on the density. The model is tested against simulations, against data on amylopectin, a major component of starch, on glycogen, and on polyglycerols. For samples of synthetic polyglycerol and glycogen, our model holds well for all the available data. The model reveals higher-level scaling structure in glycogen, related to the β particles seen in electron microscopy.

Hyperbranched polymers have many short chains linked together. Examples include amylopectin (AP) (a major component of starch) [1], glycogen (the same chemical composition as AP but more random in its branching structure [2]), and synthetic polyglycerols [3]. We propose a physical model for the average, radial, density profiles of randomly hyperbranched polymers of given mass, which fits experimental data for these three examples. Our treatment does not model synthesis, but rather comparison of the calculated random structure to experiment shows where correlations are important. The experiments we seek to understand separate polymers by their hydrodynamic volume [4,5], such as size-exclusion chromatography (SEC) and field-flow fractionation. Detectors in line with the separation column give number and mass distributions with hydrodynamic volume, and also radii of gyration. Our model does not predict distributions of mass or size, but rather the scaling of size with mass.

Many models for hyperbranched polymers assume regular architectures, some of which are discussed in Ref. [6]. de Gennes and Hervet predicted the relation between mass and radius of a dendrimer [7]. They considered some disorder, and found power laws for growth with molecular weight. Later approaches allowed the structure to reach equilibrium [8–11]. In particular, Zook and Pickett revisited the original treatment by de Gennes and Hervet, and obtained more realistic structures [12]. Our model has new features that appear because our structures are much more disordered, as branch points are made entirely at random, rather than regularly spaced as for a dendrimer. We have neglected a variety of effects, particularly electrostatics. We show below that despite its simplicity the model agrees with experiments, but we also show where it breaks down.

Hyperbranched polymers are made up of monomers with one *A* group and more than one *B* group. Links in the polymer are all of the form *A*-*B*, so that any hyperbranched polymer has one free *A* group and many free *B* groups [13]. Our model hyperbranched polymer is assembled from simple units, such as linear chains, attached to each other randomly. This assembly of the polymer does not model synthesis; it is a means of randomly arranging branch points. The simple units themselves have one free *A* group and many free *B* groups, and fluctuate in conformation, so that their description as an average density profile is justified. In the simplest version of the model, each unit is a random walk, of step length τl, where l is the length of a single monomer. We assume for simplicity τ is constant for any given polymer. This simplest version of our model is inspired by experiments in which an enzyme is added to AP and glycogen that snips each branch point with 100% efficiency. One application of our model is to reassemble theoretically this "debranched" distribution of chains and to compare to real AP or glycogen (see Fig. 3 below). We start from one walk, and add others, each time choosing a new branch point at random. Simulations based on this model have been published elsewhere [14,15]. Here we describe a much more general analytic approach: we can build up our hyperbranched polymer from simple units which may have any internal branching structure [6]. We attach each new unit's single, free *A* group to one of the *B* groups in the polymer already, chosen at random, then the new unit's *B* groups are available for further addition.

References [13,16,17] calculate the number- and weight-average molecular weights of randomly hyperbranched polymers, among other quantities. Our work differs in that we are not distributing monomers between polymers, but considering the ensemble-average growth of a single polymer, and more importantly in that we are introducing the effects of forbidden monomer overlap. Each polymer in this ensemble has the same mass, and we increase this mass, calculating its effect on the polymer size.

There are two contributions to the probability of successful addition of a new unit to the polymer. The first is the need to attach to a monomer: the probability of addition at some point **R** will increase with the density at **R**. The point **R** is the point at which a new unit's *A* group attaches to one of the existing polymer's *B* groups, and the function $\zeta(\mathbf{r} - \mathbf{R})$ describes that new unit's distribution of *B* groups that are then available for further addition. The second

contribution is the availability of physical space to accommodate the new unit, and the higher the density at $\mathbf{R}$ the more likely it is that addition will fail. At first neglect the second contribution, so that every free branch point is equally likely to accommodate the next simple unit. The probability of the $(N+1)$th unit attaching at the point $\mathbf{R}$ is proportional to the density $\rho(\mathbf{R}, N)$. The change in density of available B groups at $\mathbf{r}$ on formation of an A-B link at $\mathbf{R}$ is $\zeta(\mathbf{r}-\mathbf{R})$. The function ζ is Gaussian, with variance σ^2. We integrate over all possible addition sites, and normalize (NB: $\int \rho(\mathbf{r}, N) d\mathbf{r} = N$), to obtain

$$\frac{\partial \rho(\mathbf{r}, N)}{\partial N} = \frac{1}{N} \int \rho(\mathbf{R}, N) \zeta(\mathbf{r} - \mathbf{R}) d\mathbf{R} = \frac{1}{N} \rho \circ \zeta(\mathbf{r}), \tag{1}$$

where $\circ$ denotes convolution. Taking the Fourier transform of Eq. (1) leads to $N \partial_N \hat{\rho} = \hat{\rho} \hat{\zeta}$, where $\hat{f}(q)$ is the three-dimensional Fourier transform of $f(r)$. We can also permit the sizes of the simple units to vary, and for simplicity assume that σ^2 follows an exponential distribution (a restriction which will be lifted in a later paper). If the units are themselves simple (unbranched) chains in a θ solvent then this is equivalent to exponentially distributed simple chain lengths, shown to be a moderate approximation for AP [18]. In practice the exact shape of the distribution does not greatly affect our results, so we use the exponential distribution for all calculations.

We can rearrange the Fourier transform of Eq. (1) and take the average over the distribution of σ^2 to obtain

$$\frac{\partial \langle \log \hat{\rho} \rangle}{\partial \log N} = \langle \hat{\zeta} \rangle \Rightarrow \exp\langle \log \hat{\rho} \rangle = \hat{\rho}_1 N^{\langle \hat{\zeta} \rangle}, \tag{2}$$

where $\hat{\rho}_1$ is the value of $\hat{\rho}(q)$ at $N = 1$. The moments of ρ are obtained from $\hat{\rho}$ by differentiation [19],

$$r_g^2 = \langle r^2 \rangle_\rho = -\frac{\nabla_\mathbf{q}^2 \hat{\rho}(q, N)|_{q=0}}{\hat{\rho}(0, N)} = r_0^2 + K s^2 \log N, \tag{3}$$

where $s^2 = \langle \sigma^2 \rangle$, r is distance from the center of mass, r_g is the polymer's radius of gyration, r_0 is the initial ($N = 1$) radius of gyration, and $\langle \cdot \rangle_f$ is an average over all space with the probability density f. The constant K is 3 for Gaussian ζ and constant σ^2. If the simple units are exponentially distributed in σ^2, then we have $K = 6$. Growth as $r_g^2 \sim \log(N)$ has been predicted for dendrimers [8,11], and it is intriguing to see that the present model predicts the same behavior for a much less branched and more disordered structure.

Now we turn to the second effect: forbidden overlap (self-avoidance), also referred to as segmental crowding. Let ρ_0 be the density where no further addition is possible. We choose the overall probability that a chain will successfully add at $\mathbf{r}$ to be

$$P_N(\mathbf{r}) = \frac{1}{C} \rho(\mathbf{r}, N) \left(1 - \frac{\rho(\mathbf{r}, N)}{\rho_0}\right)^\gamma, \tag{4}$$

where C is the normalization constant given by $\int P d\mathbf{r} = 1$. This equation is chosen for its simplicity, and so that the probability of addition vanishes when $\rho = \rho_0$. For dendrimers various factors can substantially affect the conformation [20,21]. Here we are treating the simplest case possible, where Eq. (4) describes forbidden overlap of segments. More realistic interactions are left for future work, but the simulation results discussed below show that this simple form is sufficient when forbidden overlap is the only nonbonded interaction. We obtain the equation for self-avoiding polymers by replacing the factor ρ/N on the right-hand side of Eq. (1) with $P_N(\mathbf{r})$:

$$\frac{\partial \rho(\mathbf{r}, N)}{\partial N} = P_N \circ \zeta(\mathbf{r}). \tag{5}$$

This equation describes the formation of new branch points, i.e., the formation of A-B links. Where we allow the sizes of the simple units to fluctuate randomly, we numerically integrate Eq. (5) with steps of $\Delta N = 1$, selecting a new value of σ^2 from an exponential distribution at each step; this step can be made larger for cases requiring very large values of N. In the simplest treatment we put $\gamma = 1$. This choice captures most of the features of the more elaborate variants of the model, and is used for the analysis of polyglycerol and glycogen below. For calculations involving starch we use $\gamma = 5$. This choice is made to account for the length of the simple chains: each is modeled as 5 segments, each 5 monomers long. A factor of $(1 - \rho/\rho_0)$ appears for each of the five steps as the chance that it will fit, giving $\gamma = 5$.

A typical result for r_g^2 is shown in Fig. 1. Two regions of growth are apparent, with a smooth crossover from one to the other. The light polymers grow logarithmically. The heavier ones grow as a power law. If we include the random choice of simple unit sizes and forbidden overlap, then in place of the low molecular weight growth as $r_g^2 \sim \log(N)$ [Eq. (1)], we have $r_g \sim \log(N)$. The former has been seen
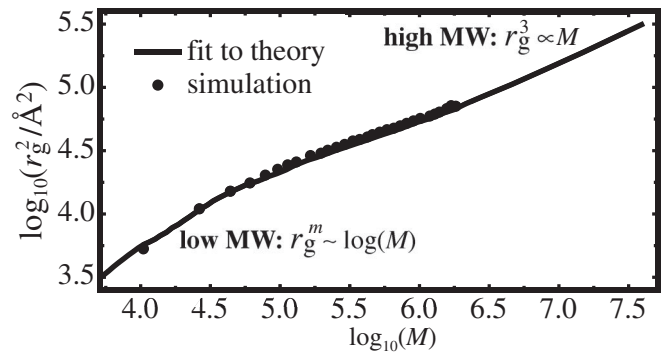

FIG. 1. A typical prediction for the radius of gyration from our model with parameters typical of a polysaccharide. If we randomly vary the sizes of units making up the polymer, we find $m = 1$ over up to three decades in mass. The points are from simulations that are described in detail in Refs. [14,15], for $\tau = 4$ (see discussion with Fig. 3 for other parameters).

for dendrimers; the latter is new as far as we know. We see this new growth for up to three decades in mass before the power law growth with $r_g^3 \propto M$ takes over. An upper bound on the radius of a dendrimer has been reported to grow as $\ln(N)$ [22].

The points in Fig. 1 are the radii of gyration of polymer chains generated in Monte Carlo simulations using methods described in detail in [14,15]. These structures are made by attaching random walks with only the constraints of hyperbranching and nonoverlapping chains. The simulations generate many structures at each mass, so that the branching structures and shapes of the randomly hyperbranched polymers are well sampled. Any single simulated structure is likely to be irregular in shape, but the ensemble-average density is spherically symmetric. The agreement between the simulations and our theory shows that the simulated fluctuating structure is well described by our equations, and that a theory for the ensemble averaged density profile is meaningful. Of course, a real polymer may have more complex structure, and disagree with our predictions, indeed we show this below, but our simple model works surprisingly well.

A hyperbranched polymer of given mass can have different structures, and a distribution of sizes. In Ref. [15], we show that this distribution is not too broad, and becomes relatively narrower as the polymer becomes larger. Our theory predicts the density profile averaged over the ensemble of possible branching structures for a given mass, and so we obtain an average r_g^2 at each mass.

Kainthan *et al.* reported triple-detection SEC of hyperbranched polyglycerols [3]. Ioan *et al.* report similar analysis for glycogen [2]. We solved Eq. (5) for the simplest case of $\gamma = 1$, taking s as the unit of length, for values of ρ_0 varying between 6×10^{-2} and 10^3. We then varied s^2 and $\bar{n}$, the average number of monomers in each simple unit, to fit each experiment to each model calculation. For all five experimental data sets, the best fit was for $\rho_0 \approx s^{-3}$. This is the density at which simple units overlap. In the fit to Monte Carlo simulations in Fig. 1 we found $\rho_0 \approx 0.9s^{-3}$. The experimental data are shown in Fig. 2 as r_g/s vs $\ln(N)$, where N is the number of units added, $N = M/(\bar{n}M_0)$, where M_0 is the mass of a monomer. All the experimental data, covering about two decades in mass overall (before scaling), lie on the same line, predicted by our model. The values of the parameters are shown in Table I. Other samples described by Kainthan *et al.* and by Ioan *et al.* show the power law growth $r_g^3 \sim M$. This behavior is also seen in our calculations at higher degrees of polymerization (see Fig. 1).

The number of monomers in each simple unit from the fit varies from $\sim 6 \times 10^3$ to 10^5. The actual linear chains in glycogen are made up of about 20 glucose units [18], but our results imply that the scaling shown in Fig. 2 is due to the assembly of much larger units. Such units, called β particles, have been observed in electron microscopy of
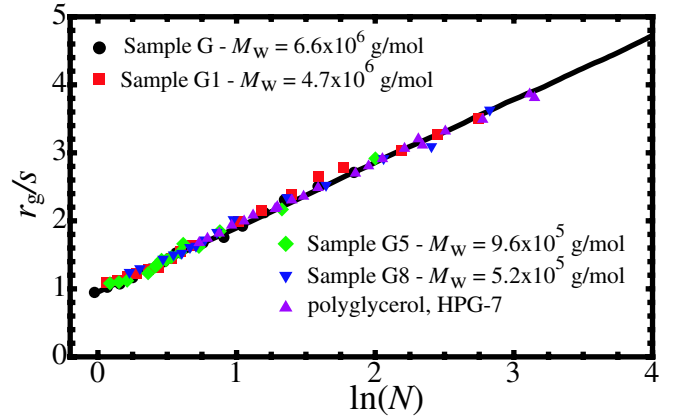

FIG. 2 (color online). Data for glycogen and polyglycerol plotted as r_g/s against $\ln(N)$ where N is the number of simple units. Each set of experimental data independently is best fit by a value of ρ_0 close to $1/s^3$. The model's prediction for this choice of ρ_0 is shown as a solid line.

glycogen [23,24]. Given the simplicity of our model, the emergence of units with sizes of the correct order of magnitude is striking. Our fits suggest diameters ($\approx 2s$) of between 20 and 50 nm (Table I), the observed β particles are around 20 to 40 nm in diameter.

Takeda *et al.* report SEC experiments on fluorescently labeled waxy (high AP) rice starch [25]. These data and the calibration used in Ref. [14] give the number and weight distributions with hydrodynamic volume [4]. The use of the calibration in [14] gives reasonable and consistent estimates of hydrodynamic volume. We take Takeda's number distribution, and combine it with our model's prediction for the mass of a polymer of given size, to obtain the mass distribution across hydrodynamic volumes. We can then test our model by comparing this mass distribution to the experimental one. We take the length of the simple chains from experimental debranched distributions to be fixed at 25 [25], the length of a monomer to have the crystallographic value 4.5 Å, and choose $\gamma = 5$. The values of $\rho_0 = 6.6 \times 10^{-3}$ nm^{-3} and $\sigma = 4.5$ nm are chosen to be by comparison to Monte Carlo simulations [15]. The value of ρ_0 is only slightly lower than the one found above for polyglycerol and glycogen, about $0.64\sigma^{-3}$. We have

TABLE I. Parameters that give the best fit of the model to the five sets of experimental data shown in Fig. 2. These values of s were obtained assuming $K = 6$ [see Eq. (3)]. A lower K implies a higher s for the same fit.

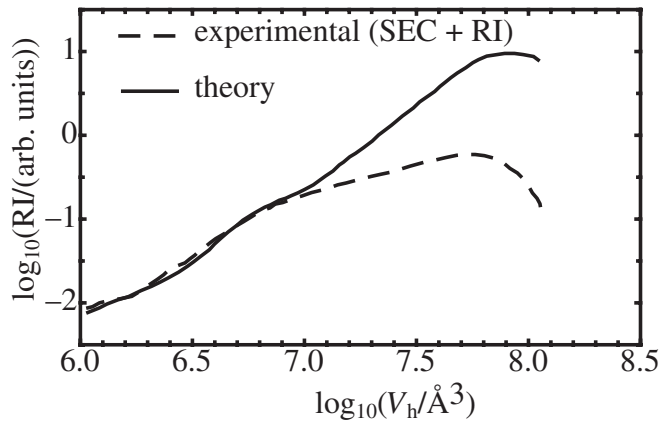| Polymer	$\bar{n}$	s (nm)
Polyglycerol HPG-7	8540	9.37
Glycogen G	92 800	25.2
Glycogen G1	35 400	18.5
Glycogen G5	10 500	13.5
Glycogen G8	6170	11.2

FIG. 3.   Comparison of our predicted weight distribution for amylopectin to that reported by Takeda *et al.* from SEC measurements [25]. Our predicted distribution is calculated from the number distribution given by Takeda *et al.*.

scaled our predicted weight distribution in Fig. 3 to match the refractive index signal. Our model and the experiment show the same (roughly power law) growth in weight distribution over about a decade in hydrodynamic volume, then they deviate. We argue that this is because the enzymatic processes in the biosynthesis are such that the branching structure in AP ceases to be quasirandom at these larger sizes, because the monomers would otherwise be too closely packed.

Our model is a very simple one, and predicts only the average radial density profile of a complex structure. It makes no attempt to predict distributions of size and neglects many effects on polymer structure. Yet it agrees with simulations, and more importantly with experimental data on three separate polymers. The agreement with the polyglycerol and glycogen data is striking, and the prediction by this fit of the existence of β particles, observed in electron microscopy, is strong evidence that our simple model captures the scaling of size with mass. Still, many fascinating issues remain to be explored: for example, we have no simple explanation for the $r_g \sim \ln(M)$ scaling which we have shown is found in experimental data as well as in our model calculations. We leave this, the exploration of more realistic interactions, and the combination of our work with that in Refs. [13,16,17], to future work.

[1] H. P. Guan and P. L. Keeling, Trends Glycosci. Glycotechnol. **10**, 307 (1998).
[2] C. E. Ioan, T. Aberle, and W. Burchard, Macromolecules **32**, 7444 (1999).
[3] R. K. Kainthan, E. B. Muliawan, S. G. Hatzikiriakos, and D. E. Brooks, Macromolecules **39**, 7708 (2006).
[4] M. Gaborieau, R. G. Gilbert, A. Gray-Weale, J. M. Hernandez, and P. Castignolles, Macromol. Theory Simul. **16**, 13 (2007).
[5] L. K. Kostanski, D. M. Keller, and A. E. J. Hamielec, J. Biochem. Biophys. Methods **58**, 159 (2004).
[6] W. Burchard and A. Thurn, Macromolecules **18**, 2072 (1985).
[7] P. G. de Gennes and H. Hervet, J. Phys. Lett. **44**, L351 (1983).
[8] D. Boris and M. Rubinstein, Macromolecules **29**, 7251 (1996).
[9] S. V. Lyulin, L. J. Evers, P. van der Schoot, A. A. Darinskii, A. V. Lyulin, and M. A. J. Michels, Macromolecules **37**, 3049 (2004).
[10] T. Mulder, A. V. Lyulin, P. van der Schoot, and M. A. J. Michels, Macromolecules **38**, 996 (2005).
[11] R. La Ferla, J. Chem. Phys. **106**, 688 (1997).
[12] T. C. Zook and G. T. Pickett, Phys. Rev. Lett. **90**, 015502 (2003).
[13] W. Burchard, Macromolecules **5**, 604 (1972).
[14] C. Watts, A. A. Gray-Weale, and R. G. Gilbert, Biomacromolecules **8**, 455 (2007).
[15] D. Konkolewicz, A. A. Gray-Weale, and R. G. Gilbert, J. Polym. Sci., Part A: Polym. Chem. (to be published).
[16] S. Erlander and D. French, J. Polym. Sci. **20**, 7 (1956).
[17] M. Gordon, G. N. Malcolm, and D. S. Butler, Proc. R. Soc. A **295**, 29 (1966).
[18] J. V. Castro, C. Dumas, H. Chiou, M. A. Fitzgerald, and R. G. Gilbert, Biomacromolecules **6**, 2248 (2005).
[19] L. E. Reichl, *A Modern Course in Statistical Physics* (John Wiley and Sons, New York, 1998), 2nd ed.
[20] P. Welch and M. Muthukumar, Macromolecules **31**, 5892 (1998).
[21] C. B. Gorman and J. C. Smith, Polymer **41**, 675 (2000).
[22] F. Ganazzoli, R. La Ferla, and G. Terragni, Macromolecules **33**, 6611 (2000).
[23] J.-L. Putaux, A. Buléon, R. Borsali, and H. Chanzy, Int. J. Biol. Macromol. **26**, 145 (1999).
[24] P. Drochmans, J. Ultrastruct. Res. **6**, 141 (1962).
[25] Y. Takeda, S. Shibahara, and I. Hanashiro, Carbohydr. Res. **338**, 471 (2003).